Investigating the outcomes of virus coinfection within and across host species

Ryan M. Imrie*[1], Sarah K. Walsh[1], Katherine E Roberts[1], Joanne Lello[2], Ben Longdon[1]

1. Centre for Ecology & Conservation, Faculty of Environment, Science, and Economy, Biosciences, University of Exeter, Penryn Campus, Penryn, United Kingdom
2. School of Biosciences, Cardiff University, Cardiff, United Kingdom

*Corresponding author: r.imrie@exeter.ac.uk

Abstract

Interactions between coinfecting pathogens have the potential to alter the course of infection and can act as a source of phenotypic variation in susceptibility between hosts. This phenotypic variation may influence the evolution of host-pathogen interactions within host species and interfere with patterns in the outcomes of infection across host species. Here, we examine experimental coinfections of two *Cripaviruses* – Cricket Paralysis Virus (CrPV), and Drosophila C Virus (DCV) – across a panel of 25 *Drosophila melanogaster* inbred lines and 47 *Drosophilidae* host species. We find that interactions between these viruses alter viral loads across *D. melanogaster* genotypes, with a ~3 fold increase in the viral load of DCV and a ~2.5 fold decrease in CrPV in coinfection compared to single infection, but we find little evidence of a host genetic basis for these effects. Across host species, we find no evidence of systematic changes in susceptibility during coinfection, with no interaction between DCV and CrPV detected in the majority of host species. These results suggest that phenotypic variation in coinfection interactions within host species can occur independently of natural host genetic variation in susceptibility, and that patterns of susceptibility across host species to single infections can be robust to the added complexity of coinfection.

Introduction

Coinfections – simultaneous infections of a host with multiple pathogen lineages or species – are ubiquitous in nature, and represent the real-world context in which many infections occur [1–3]. Interactions between pathogens during coinfection can alter the virulence experienced by the host, and the loads and transmission rates of one or both pathogens [4–9]. At a population level, these interactions can lead to changes in infectious disease dynamics [10,11], such as the exclusion of novel viruses from host populations with other established pathogens [12,13], or fluctuations in the epidemic spread of one virus depending on the prevalence of other viruses [14,15]. These changes can ultimately alter the selective pressures imposed on hosts and pathogens, and coinfections have been proposed as a mechanism for the maintenance of genetic diversity in pathogen populations; as the fitness of pathogen genotypes may fluctuate not only in red queen dynamics with the host but also with coinfection prevalence and a pathogen's competitive ability across coinfection scenarios [16]. Despite this, coinfections remain a largely understudied source of phenotypic variation during infection, and further investigation of their influence on the outcome of infection in different hosts and host species is needed.

Within coinfected hosts, pathogens can interact directly, such as through the production of toxins or modulation of the opposing pathogen's gene expression [17,18], or indirectly through the production of common goods, competition for host resources, and interactions with host gene expression and immunity [19–24]. For example, in HIV-virus coinfections – a mechanistically well studied set of interactions due to their suspected involvement in AIDS progression [25] – several viruses have been shown to alter susceptibility to HIV infection by changing the expression of cell surface receptors CD4 and CCR5 [26,27]. In the case of human cytomegalovirus (HCMV), which upregulates CCR5 expression and increases HIV viral loads in coinfected tissues, HIV can reciprocally induce the expression of transmembrane proteins that promote HCMV infection [28,29]. Conversely, measles virus coinfections can inhibit HIV-1 replication due to measles-related activation of proinflammatory cytokines [30]. As such, the presence of coinfecting viruses may enhance or interfere with the ability of a virus to effectively establish an infection in a host, with these interactions often mediated by host components.

Despite the known role of host components in many coinfections, the extent to which host genetic variation in these components can influence the strength of interactions between pathogens – and so the ability of hosts to evolve directly to selective pressures imposed by coinfection – is unknown. Evidence suggesting a role of host genetics in the outcomes of coinfections is limited; however, several studies in plants have shown that pathogen community composition, coinfection prevalence, and disease severity during coinfection can vary non-randomly between host genotypes [31–33]. Coinfections can also be influenced by host dietary choices and the quantity of nutrients available in the host [34,35] – both of which are heritable traits [36,37] – which suggests that host genetic variation may influence coinfection outcomes. Broadly, we may expect host genetic variation to lead to changes in the strength of interaction between coinfecting pathogens when the interaction occurs through modulation of a host component (e.g., immune pathways or resource competition), or when host genetic variation influences the pathogen load of one or both pathogens.

Variation in the outcomes of coinfection across host species has also received relatively little attention, with most comparative cross-species studies focusing either on single infections in controlled experimental systems [38–45] or looking for broad patterns in infections across large datasets of natural systems where coinfection status is unknown [46–52]. These studies have shown that the evolutionary relationships between host species can explain a large proportion of the variation in infection traits. For example, virulence tends to increase [45–47], and onward transmission and pathogen load decrease [39,46], with greater evolutionary distance between donor and recipient hosts. Irrespective of distance to the donor host, closely related species also tend to share similar levels of susceptibility to novel pathogens [39–41]. Phylogenetic models such as these form part of the growing field of zoonotic risk prediction, the aim of which is to provide accurate, actionable predictions of host-virus interactions to inform public health measures [53]. The accuracy of current models may be improved by identifying and incorporating additional sources of variation in the outcome of cross-species transmission [54]. Coinfection status, detectable through metagenomic screening [55], may be a beneficial inclusion in such models, provided the strength and/or direction of coinfection interactions are known (or inferable).

Here, we investigate the influence of coinfection on virus susceptibility within and across host species, using panels of *Drosophila* hosts and experimental infections with two

Cripaviruses: Cricket Paralysis Virus (CrPV) and Drosophila C Virus (DCV). Viral loads were measured during single and coinfection conditions across 25 inbred lines of *Drosophila melanogaster* and 47 *Drosophilidae* species. By analysing both viral loads and the change in viral loads from single to coinfection, we quantify the host genetic and phylogenetic components of susceptibility to each virus, and investigate whether these host components also influence the strength and direction of coinfection interactions in this system.

Both DCV and CrPV are well studied pathogens in *Drosophila melanogaster* and multiple similarities exist in their interactions with their hosts that could lead to interactions during coinfection. Both viruses are targeted by the antiviral RNAi pathway during infection of *D. melanogaster [56,57]*, and activate the IMD immune signalling pathway, inducing non-specific antiviral gene expression [58–60]. Each encodes an inhibitor of antiviral RNAi, which act on different components of the pathway; the DCV inhibitor binds and sequesters viral RNA to prevent its cleavage by the antiviral RNAi endonuclease *Dicer-2*, and also disrupts formation of the RNA-induced silencing complex (RISC) [61,62]; the CrPV inhibitor binds the RISC protein *Argonaute-2*, causing suppression of RISC viral RNA cleavage [62]. Infections with DCV have also been shown to induce nutritional stress in infected hosts, due to intestinal obstruction and accumulation of food in the fly crop, although CrPV infection results in no such phenotype [63]. DCV and CrPV may therefore be capable of interacting indirectly during coinfection through multiple routes: by suppression of antiviral RNAi, transactivation of host antiviral gene expression, or competition for limited host resources.

Susceptibility to DCV infection has a strong host genetic component [64], with polymorphisms in two major-effect genes (*pastrel* and *Ubc-E2H*) explaining a large proportion of the variation in DCV susceptibility [64–67]. Both genes have also been implicated in CrPV susceptibility during knockdown experiments [67]. DCV and CrPV both vary widely in their ability to persist and replicate across different *Drosophilidae* host species, with the host phylogeny explaining a large proportion of the variation in viral load during single infection [40,41]. A role of host genetics during coinfection may therefore manifest either as a change in the genetic/phylogenetic components of susceptibility to each individual virus, or as a genetic/phylogenetic component directly influencing the strength of interaction between these viruses, both of which we investigate here.

Materials & Methods

Fly stocks

Stocks of DGRP flies were kindly provided by Jon Day and Francis Jiggins [64]. In total, 25 DGRP lines were used (for details see Supplementary Table 1), with 15 lines containing the resistant "G" allele of the A2469G *pastrel* SNP and 10 containing the susceptible "A" allele [65]. *Pastrel* allele status was confirmed via conventional PCR using SNP genotyping primers from [65] (Supplementary Table 2). Laboratory stocks of 47 *Drosophilidae* host species were used to provide the across-species host panel (Supplementary Table 3), as in previous studies [40,41].

All flies were maintained in multi-generation stock bottles (Fisherbrand) at 22°C, 70% relative humidity in a 12-hour light-dark cycle. Each stock bottle contained 50ml of one of four varieties of *Drosophila* media (https://doi.org/10.6084/m9.figshare.21590724.v1) which were chosen to optimise rearing conditions for parental flies. All fly lines and species were confirmed to be negative for infection with CrPV and DCV prior to experiments by quantitative reverse-transcription PCR (qRT-PCR, described below). To limit the effects of variation in larval density on the condition of DGRP lines, experimental flies were reared in vials with finite numbers of larvae, achieved by transferring groups of five 7 day old mated females to fresh vials each day for 3 days, with daily pools of offspring from these vials collected for experiments. Due to large differences in fecundity, larval density controls were not practical for the across-species host panel.

Inferring the Drosophilidae host phylogeny

The method used to infer the host phylogeny has been described in detail elsewhere [40]. Briefly, publicly available sequences of the *28S*, *Adh*, *Amyrel*, *COI*, *COII*, *RpL32*, and *SOD* genes were collected from Genbank (see https://doi.org/10.6084/m9.figshare.13079366.v1 for a full breakdown of genes and accessions by species). Gene sequences were aligned in Geneious version 9.1.8 (https://www.geneious.com) using a progressive pairwise global alignment algorithm with free end gaps and a 70% similarity IUB cost matrix. Gap open penalties, gap extension penalties, and refinement iterations were kept as default.

Phylogenetic reconstruction was performed using BEAST version 1.10.4 [68], as the subsequent phylogenetic mixed model (described below) requires a tree with the same root-tip distances for all taxa. Genes were partitioned into separate ribosomal (*28S*), mitochondrial (*COI*, *COII*), and nuclear (*Adh*, *Amyrel*, *RpL32*, *SOD*) groups. The mitochondrial and nuclear groups were further partitioned into groups for codon position 1+2 and codon position 3, with unlinked substitution rates and base frequencies across codon positions. Each group was fitted to separate relaxed uncorrelated lognormal molecular clock models using random starting trees and four-category gamma-distributed HKY substitution models. The BEAST analysis was run twice, with 1 billion Markov chain Monte Carlo (MCMC) generations sampled every 100,000 iterations, using a birth-death process tree-shape prior. Model trace files were evaluated for chain convergence, sampling, and autocorrelation using Tracer version 1.7.1 [69]. A maximum clade credibility tree was inferred from the posterior sample with a 10% burn-in. The reconstructed tree was visualised using ggtree version 2.0.4 [70].

Virus isolates

Virus stocks were kindly provided by Julien Martinez (DCV) [71], and Valérie Dorey and Maria Carla Saleh (CrPV) [61]. The DCV isolate used here (DCV-C) was isolated from lab stocks established by wild capture in Charolles, France [72], and the CrPV isolate was collected from *Teleogryllus commodus* in Victoria, Australia [73]. Virus stocks were checked for contamination with CrPV (DCV) and DCV (CrPV) by qRT-PCR and diluted in Ringers solution [74] to equalise the relative concentrations of viral RNA. Before inoculation, virus aliquots were either mixed 1:1 with Ringers (single infection inoculum) or 1:1 with an aliquot of the other virus (coinfection inoculum). This was done to keep the individual doses of each virus consistent between infection conditions.

Inoculation

Before inoculation, 0-1 day old male flies were transferred to vials containing cornmeal media. These flies were then transferred to fresh media every 2 days for a week (age 7-8 days), at which point they were inoculated. Vials contained between 7 and 20 flies (mean = 12.7), and were kept at 22°C, 70% relative humidity in a 12-hour light-dark cycle throughout the experiments. Male flies were used to avoid any effect of sex or mating status, which has

been shown to influence the susceptibility of female flies to other pathogens [75–77]. Flies were inoculated under CO_2 anaesthesia via septic pin prick with 12.5µm diameter stainless steel needles (Fine Science Tools, CA, USA). These needles were bent approximately 250µm from the end to provide a depth stop and dipped in virus inoculum before being pricked into the pleural suture of anaesthetised flies. Inoculation by this method bypasses the gut immune barrier but avoids differences in inoculation dose due to variation in feeding rate, and infections using this route largely follow the same course as oral infections but with less stochasticity [78].

Measuring change in viral load

To provide a measure of viral load during single and coinfection, inoculated flies were snap frozen in liquid nitrogen at 2 days (± 2 hours) post-inoculation. Additional samples were collected for each species in the *Drosophilidae* host panel immediately after inoculation, which were used to account for differences in housekeeping gene expression across host species during C_T normalisation (see below). Total RNA was extracted from flies homogenized in Trizol (Invitrogen) using chloroform-isopropanol extraction, and reverse transcribed using GoScript reverse transcriptase (Promega) with random hexamer primers. qRT-PCR was carried out on 1:2 diluted cDNA on an Applied Biosystems StepOnePlus system using a Sensifast Hi-Rox SYBR kit (Bioline). Cycle conditions were as follows: initial denaturation at 95°C for 120 seconds, then 40 cycles of 95°C for 5 seconds and 60°C for 30 seconds. The primer pairs used for virus qRT-PCR assays were: (DCV) forward, 5'-GACACTGCCTTTGATTAG-3'; reverse, 5'-CCCTCTGGGAACTAAATG-3'; (CrPV) forward, 5'-TTGGCGTGGTAGTATGCGTAT-3'; reverse, 5'-TGTTCCGTCCTGCGTCTC. RPL32 housekeeping gene primers were used for normalisation and varied by species (Supplementary Table 4-5). For each biological sample, two technical replicate qRT-PCR reactions were performed for each amplicon (viral and RPL32).

Between-plate variation in C_T values was estimated and corrected using linear models with plate ID and biological replicate ID as fixed-effects [79,80]. For DGRP lines, mean viral C_T values from technical replicate pairs were normalised to RPL32 and converted to relative viral load using the $\Delta\Delta C_T$ method, where $\Delta C_T = C_{T:Virus} - C_{T:RPL32}$ and $\Delta\Delta C_T = 40 - \Delta C_T$. To account for potential differences in RPL32 expression between species, change in viral load in the *Drosophilidae* species experiment was calculated as fold-change in viral load from

inoculation to 2 days post-infection using the $\Delta\Delta C_T$ method, where $\Delta C_T = C_{T:Virus} - C_{T:RPL32}$ and $\Delta\Delta C_T = \Delta C_{T:day0} - \Delta C_{T:day2}$. Amplification of the correct products was verified by melt curve analysis. Repeated failure to amplify product, the presence of melt curve contaminants, or departures from the melt curve peaks of positive samples (±1.5°C for viral amplicons; ±3°C for RPL32) were used as exclusion criteria for biological replicates. For a full breakdown of the replicates per experiment for each combination of fly line/species and infection condition see Supplementary Table 6.

Analysis of coinfection within and across species

Genetic variation in the outcome of single and coinfection across DGRP lines was analysed using methods previously described by Magwire et al. [64]. Briefly, multivariate generalised linear mixed models (GLMMs) were fitted using the R package MCMCglmm [81], with either the viral loads of each virus under each infection condition, or the change in viral load during coinfection (coinfection viral load - single infection viral load) as the response variable. The structures of these models were as follows:

$$y_{lic} = \beta_{1:c} + \mu_{l:c} + \mu_{b:c} + e_{lic} \quad (1)$$

$$y_{liv} = \beta_{1:v} + \mu_{l:v} + \mu_{b:v} + e_{liv} \quad (2)$$

In model (1), y_{lic} is the viral load for the combination of virus and infection condition c (CrPV single infection, CrPV coinfection, DCV single infection, DCV coinfection) in the i^{th} biological replicate of DGRP line l. The fixed effect β_1 represents the intercepts for each combination, the random effect μ_l represents the deviation of each DGRP line from the overall mean viral load for each combination (equivalent to the between-line variance), and e_{lic} represents the residual error. A small but significant effect of experiment block was found in initial models, driven by ~10 fold differences in DCV viral loads of the third experimental block. To account for this, random effects of block by infection condition ($\mu_{b:c}$, $\mu_{b:v}$) were added to both models. The structure of model (2) remains the same, but with the change in viral load during coinfection for each virus as the response variable, and y_{liv} representing the change in viral load for the i^{th} biological replicate of virus v and DGRP line l. *Pastrel* allele status (susceptible “A”, resistant “G”) was included in additional models as a fixed effect ($\beta_{2:lp}$).

253 Phylogenetic GLMMs were used to investigate the effects of host evolutionary relatedness
254 on viral load during single and coinfection, and to calculate interspecific correlations between
255 different infection conditions across host species. Multivariate models were fitted with the
256 viral loads of each virus under each infection condition as the response variable. The
257 structure of these models were as follows:

$$y_{hic} = \beta_{1:c} + \mu_{p:hc} + \mu_{s:hc} + e_{hic} \quad (3)$$

$$y_{hic} = \beta_{1:c} + \mu_{p:hc} + e_{hic} \quad (4)$$

258

259 In these models, y_{hic} is the change in viral load for the combination of virus and infection
260 condition *c* (CrPV single infection, CrPV coinfection, DCV single infection, or DCV
261 coinfection) in the i^{th} biological replicate of host species *h*. The fixed effect β_1 represents the
262 intercepts for each combination, the random effect μ_p represents the effects of the host
263 phylogeny assuming a Brownian motion model of evolution, and *e* represents the model
264 residuals. Model (3) also includes a species-specific random effect that is independent of the
265 host phylogeny ($\mu_{s:hc}$). This explicitly estimates the non-phylogenetic component of between-
266 species variance and allows the proportion of variance explained by the host phylogeny to
267 be calculated. $\mu_{s:hc}$ was removed from model (4) as model (3) struggled to separate the
268 phylogenetic and species-specific traits for some infection conditions. Wing size, measured
269 as the length of the IV longitudinal vein from the tip of the proximal segment to the join of the
270 distal segment with vein V [82], provided a proxy for body size [83] and was included in a
271 further model as a fixed effect ($wingsize\beta_{2:hc}$). This was done to ensure that any phylogenetic
272 signal in body size did not explain the differences seen in viral load between species [84].

273

274 To investigate the effect of host evolutionary relatedness on the change in viral load from
275 single to coinfection, additional models were run with the change in viral load during
276 coinfection (coinfection viral load - single infection viral load) on viral load as the response
277 variable:

$$y_{hiv} = \beta_{1:v} + \mu_{p:hv} + \mu_{s:hv} + e_{hiv} \quad (5)$$

$$y_{hiv} = \beta_{1:v} + \mu_{p:hv} + e_{hiv} \quad (6)$$

278

In these models, y_{hiv} is the change in viral load for the i^{th} biological replicate of virus *v* and host species *h*. The explanatory structure otherwise remains the same as models (3-4).

Within models (1-6), the random effects and residuals were assumed to follow a multivariate normal distribution and a centred mean of 0. Models (1-2) were fitted with a covariance structure $V_t \otimes I$ for the between line variances, and $V_e \otimes I$ for the residuals, with $\otimes$ representing the Kronecker product, and *I* representing an identity matrix. *V* represents 4 x 4 covariance matrices for model (1) and 2 x 2 covariance matrices for model (2) which describe the between-line variances and covariances in viral load for each infection condition and virus. Models (3-6) were fitted with a covariance structure of $V_p \otimes A$ for the phylogenetic effects, $V_s \otimes I$ for species-specific effects, and $V_e \otimes I$ for residuals. *A* represents the host phylogenetic relatedness matrix, *I* an identity matrix, and *V* represents 4 × 4 covariance matrices for models (3-4), or 2 x 2 covariance matrices for models (5-6), describing the between-species variances and covariances of changes in viral load for each combination of virus and infection condition. As each biological replicate was only tested with one combination of virus and infection condition, the covariances of V_e cannot be estimated and were set to 0 for all models.

Models were run for 13 million MCMC iterations, sampled every 5000 iterations with a burn-in of 3 million iterations. Parameter expanded priors were placed on the covariance matrices, resulting in multivariate F distributions with marginal variance distributions scaled by 1000. Inverse-gamma priors were placed on the residual variances, with a shape and scale equal to 0.002. To ensure the model outputs were robust to changes in prior distribution, models were also fitted with flat and inverse-Wishart priors, which gave qualitatively similar results. All parameter estimates reported from models (1-6) are means of the posterior density, and 95% credible intervals (CIs) are the 95% highest posterior density intervals which are reported in brackets following the estimates in the results.

The covariance matrices of models (1) and (2) were used to calculate the heritabilities (h^2), and covariates of additive genetic and environmental variation (CV_A and CV_E respectively) of viral load and the effects of coinfection within host species. Heritability was calculated as $h^2 = \frac{V_A}{V_A + V_E}$, where V_A represents the additive genetic variance and V_E the environmental

variance of each trait [85]. As DGRP lines are homozygous, V_A can be calculated as half the between-line variance, assuming purely additive genetic variation [64]. V_E was set as the residual variance of each model, which contains both non-additive genetic and environmental effects on viral load and any measurement errors. Genetic correlations between infection conditions were calculated from the model (1) and (2) v_I matrices as $\frac{cov_{x,y}}{\sqrt{var_x \times var_y}}$ and slopes of each relationship as $\frac{cov_{x,y}}{var_x}$.

The proportion of the between species variance that can be explained by the phylogeny was calculated from models (3) and (5) using the equation $\frac{V_p}{V_p + V_s}$, where v_p and v_s represent the phylogenetic and species-specific components of between-species variance respectively [84], and are equivalent to phylogenetic heritability or Pagel's lambda [86,87]. The repeatability of viral load measurements was calculated from models (4) and (6) as $\frac{V_p}{V_p + V_e}$, where v_e is the residual variance of the model [88]. Interspecific correlations in viral load between single and coinfection were calculated from model (4) v_p matrix as $\frac{cov_{x,y}}{\sqrt{var_x \times var_y}}$.

Data Availability

Data and R scripts for all included statistical models can be found at https://doi.org/10.6084/m9.figshare.21657503.v1.

Results

Coinfection causes changes in DCV and CrPV viral load across D. melanogaster genotypes

To investigate variation in the outcome of coinfection within host species, we injected a total of 8,618 flies from 25 lines of the Drosophila Genetic Reference Panel with one of three virus inoculums: DCV, CrPV, and DCV + CrPV, and measured the outcome of infection as the viral load of each virus at 2 days post-inoculation using qRT-PCR (Fig. 1). Point estimates of the mean viral load across lines suggest that DCV viral load increases ~3-fold during coinfection with CrPV, and CrPV viral load decreases ~2.5-fold during coinfection with DCV, although credible intervals of these estimates overlapped (Table 1). When models were fitted on the change in viral load (coinfection - single infection), in effect treating viral loads

within experiment blocks as paired data, similar and significant effects of coinfection across lines were detected (Table 1). Several lines showed notably large changes during coinfection: two DGRP lines showed ~10 fold decreases in CrPV viral load, and three lines showed ~40-150 fold increases in DCV viral load. Removing these lines from model (2) reduced the mean changes in viral load during coinfection to a ~2 fold increase for DCV and a ~2 fold decrease for CrPV, but the effects of coinfection on both viruses remained significant.

Figure 1: Viral loads of CrPV and DCV across DGRP lines during single and coinfection. Bar heights show the mean viral load or changes in viral load (coinfection - single infection) at 2 dpi on a log_{10} scale, with error bars showing the standard error of the mean. Blue bars represent single infection viral loads, or changes in viral load where single infection viral loads were greater than coinfection viral loads. Red bars represent coinfection viral loads, or changes in viral load where coinfection viral loads were greater than single infection viral loads. DGRP lines are arranged on the x-axis in order of susceptibility to CrPV during single infection.

No evidence of a host genetic component to the outcome of coinfection

To estimate the influence of host genetic variation on the viral loads measured during single and coinfection, GLMMs were fitted to allow the phenotypic variation in viral loads to be partitioned into genetic and environmental components. Point estimates of the heritability of DCV viral load (0.25-0.30) were higher than for CrPV (0.13), and this difference was driven by changes in the genetic component of variation (Supplementary Table 7): CrPV CV_A = 0.08, (0.05, 0.11), DCV CV_A = 0.16, (0.12, 0.20). This is consistent with previous studies which also found the genetic component of variation in susceptibility of *D. melanogaster* to single infections with DCV (a natural pathogen) is higher than for CrPV (a novel pathogen) [64]. However, we found little evidence that heritability of DCV or CrPV viral loads change in relation to coinfection, with the credible intervals of h^2 estimates for single and coinfection viral loads overlapping for both viruses (Table 1). Additionally, no host genetic component was found for the change in viral load during coinfection (Table 1, Supplementary Table 8). Together, this suggests that variation in the strength of coinfection interactions between these viruses was independent of host genetic variation, and that coinfection status does not appear to alter the host genetic component of susceptibility to either virus.

Correspondingly, strong positive correlations between single and coinfection viral loads were found for both DCV: r = 0.94 (0.84, 1.00), and CrPV: r = 0.90 (0.73, 1.00), with little evidence of genotype-by-coinfection interactions. Strong positive correlations were also seen between the two viruses, such that DGRP lines more susceptible to DCV were often also more susceptible to CrPV (Fig 2). Together, this suggests that susceptibility to DCV and CrPV share similar genetic architectures within *D. melanogaster*, with host genetic variation affecting DCV viral load similarly affecting CrPV viral load, again irrespective of coinfection status.

Table 1: Estimates of the phenotypic mean, environmental variance (V_E), additive genetic variance (V_A), and heritability (h^2) of viral load and the change in viral load during coinfection across DGRP lines for CrPV and DCV during single infection and coinfection. Values for "single infection" and "coinfection" conditions were taken from model (1), which was fitted on $\log_{10}$-transformed fold-changes in viral load, while values for "change" were taken from model (2), which was fitted on $\log_{10}$-transformed Δ fold-changes in viral load (coinfection - single infection).

Virus	Condition	Mean	V_e	V_A	h^2
CrPV	Single Infection	4.68 (4.02, 5.34)	0.94 (0.79, 1.09)	0.14 (0.05, 0.25)	0.13 (0.05, 0.22)
	Coinfection	4.28 (3.60, 4.96)	0.74 (0.61, 0.86)	0.12 (0.04, 0.20)	0.13 (0.06, 0.22)
	Change	-0.27 (-0.37, -0.18)	0.23 (0.15, 0.27)	0.00 (0.00, 0.02)	0.02 (0.00, 0.09)
DCV	Single Infection	6.17 (5.29, 6.98)	2.08 (1.75, 2.46)	1.00 (0.47, 1.65)	0.32 (0.20, 0.46)
	Coinfection	6.62 (5.82, 7.40)	1.80 (1.49, 2.09)	0.71 (0.33, 1.18)	0.28 (0.16, 0.40)
	Change	0.33 (0.18, 0.47)	0.21 (0.15, 0.27)	0.03 (0.00, 0.06)	0.11 (0.00, 0.23)

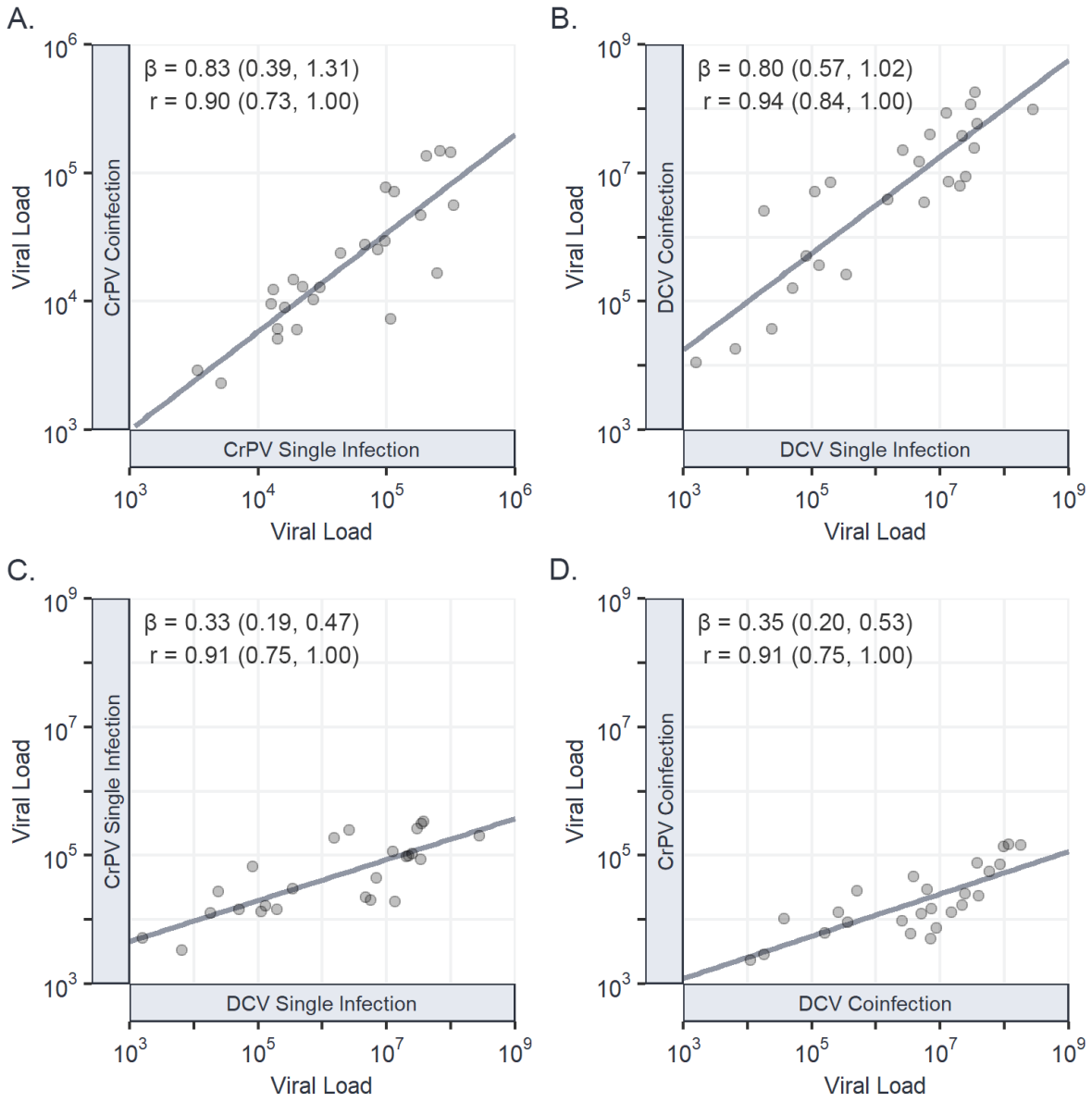

Figure 2: Genetic correlations in viral load between single and coinfections of CrPV and DCV. Correlations in viral load between CrPV during single and coinfection (A); DCV during single and coinfection (B); CrPV and DCV during single infection (C); and CrPV and DCV during coinfection (D). Individual points represent the mean viral load at 2 dpi for each DGRP line on a $\log_{10}$ scale, with trend lines added from a univariate least-squares linear model for illustrative purposes. Genetic correlations (r), regression slopes (β), and 95% CIs have been taken from the output of model (1).

Viral load remains a repeatable trait across host species during coinfection

To investigate how coinfection may alter susceptibility across host species, we performed similar experimental single and coinfections across 47 *Drosophilidae* host species. A total of

13,596 flies were inoculated, and the change in viral load after two days of infection was measured by qRT-PCR (Fig 3). Neither virus showed evidence of changes in their overall mean viral loads or variance across host species between single and coinfection (Table 2). Power analysis based on the effects of coinfection found in *D. melanogaster* (Fig. 1, Supplementary Methods) showed that the level of replication in this experiment was adequate to detect systematic ~2-fold changes in viral load across host species. As such, this result suggests there is no evidence for large additive effects of coinfection that are consistent across host species. Instead, most host species showed no discernible differences in viral loads during coinfection, with notable exceptions including *D. obscura* (both viruses decreased in viral load by ~600 fold), *D. suzukii* (DCV unchanged but CrPV decreased by ~25 fold), *Zaprionus tuberculatus* (CrPV unchanged but DCV decreased by ~50 fold), and *D. virilis* (CrPV unchanged but DCV increased by ~40 fold).

Phylogenetic GLMMs were fitted to the data to determine the proportion of variation in viral load explained by the host phylogeny (Table 2). The host phylogeny explained a large proportion of the variation in viral load for CrPV during single infection: 0.88 (0.69, 1), and coinfection: 0.82 (0.59, 1), with no credible difference between these two estimates. Estimates of the variation in DCV viral load explained by phylogeny were low: 0.1-0.13 with wide credible intervals due to model (3) struggling to separate phylogenetic and non-phylogenetic effects for DCV. The repeatability of viral load across host species was high for both viruses during single infection, CrPV: 0.86 (0.78, 0.93), DCV: 0.94 (0.90, 0.97) and coinfection, CrPV: 0.76 (0.64, 0.87), DCV: 0.89 (0.82, 0.94), with the between-species phylogenetic component explaining a high proportion of the variation in viral load with little within-species variation or measurement error. Although point estimates of these parameters were all consistent with a slight decrease in phylogenetic signal during coinfection, the effect size was small, and we did not detect credible differences in phylogenetic signal between single and coinfection.

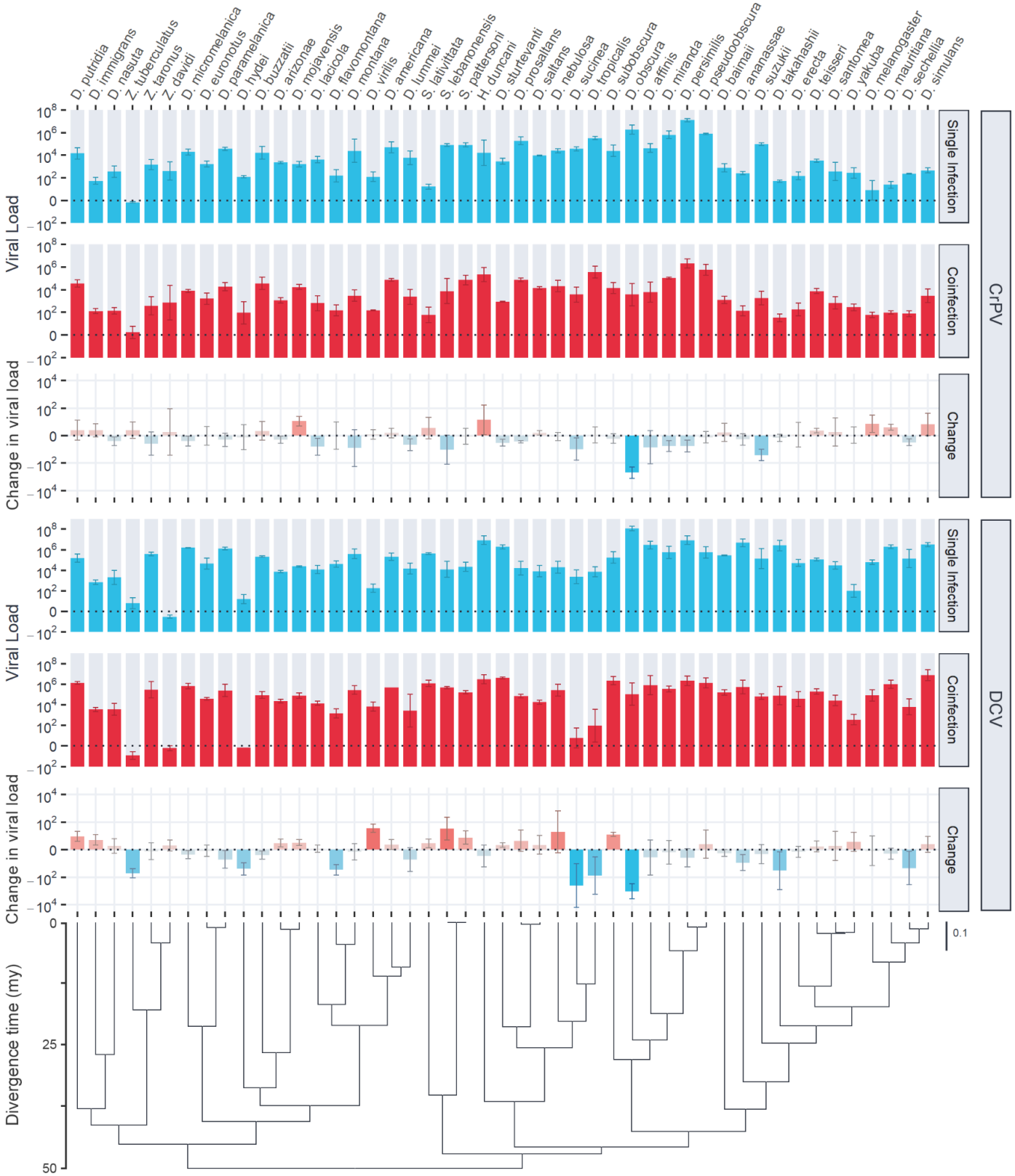

Figure 3: Viral loads of CrPV and DCV across host species during single and coinfection. Bar heights show the mean viral load or changes in viral load (coinfection – single infection) by 2 dpi on a $\log_{10}$ scale, with error bars showing the standard error of the mean. Blue bars represent single infection viral loads, or changes in viral load where single infection viral loads were greater than coinfection. Red bars represent coinfection viral loads, or changes in viral load where coinfection viral loads were greater than single infection. The phylogeny of *Drosophilidae* hosts is presented at the bottom, with the scale bar showing nucleotide substitutions per site, and the axis showing the approximate age since divergence in millions of years (mya) based on estimates from [89].

Table 2: Estimates of overall mean, across-species variance, repeatability, and the proportion of variance explained by the host phylogeny for viral load and the change in viral load during coinfection. Values for mean viral load, across species variance, and repeatability for the "single infection" and "coinfection" conditions were taken from model (4), which was fitted on $\log_{10}$-transformed fold-changes in viral load, while these values for "change" during coinfection were taken from model (6), which was fitted on $\log_{10}$-transformed Δ fold-changes in viral load (coinfection - single infection). The proportion of variance explained by phylogeny was taken from model (3) for the "single infection" and "coinfection" conditions, and model (5) for "change" during coinfection.

Virus	Condition	Mean	Across-species variance	Repeatability	Variance explained by phylogeny
CrPV	Single Infection	3.44 (1.88, 4.99)	3.63 (1.86, 5.75)	0.86 (0.78, 0.93)	0.88 (0.69, 1)
	Coinfection	3.30 (2.21, 4.38)	2.93 (1.36, 4.75)	0.76 (0.64, 0.87)	0.82 (0.59, 1)
	Change	-0.13 (-0.49, 0.19)	0.17 (0, 0.46)	0.11 (0, 0.27)	0.57 (0, 1)
DCV	Single Infection	4.75 (2.09, 7.49)	9.85 (5.20, 15.46)	0.94 (0.90, 0.97)	0.13 (0, 0.43)
	Coinfection	4.57 (1.82, 7.26)	10.40 (4.87, 16.44	0.89 (0.82, 0.94)	0.10 (0, 0.27)
	Change	-0.12 (-1.08, 0.86)	0.92 (0, 1.84)	0.36 (0.08, 0.62)	0.49 (0, 0.99)

Viral load is strongly correlated between single and coinfection across host species

Interspecific correlations in viral load between single and coinfection were calculated for each virus from the variance-covariance matrix of model (4). We found strong positive correlations in viral loads between single and coinfection for DCV: r = 0.95 (0.89, 0.99) (Fig 4A) and CrPV: r = 0.94 (0.86, 0.99) (Fig 4B), with the regression slopes of each indicating a near 1:1 relationship: DCV: β = 0.98 (0.77, 1.22), CrPV: β = 0.85 (0.66, 1.05), and limited evidence of host species by coinfection interactions. The strength of the interspecific correlation in viral load between DCV and CrPV (Fig. 4C, D) also did not differ between single: r = 0.59 (0.31, 0.82), and coinfection: r = 0.67 (0.43, 0.88) and was consistent with previous estimates: r = 0.59 (0.26, 0.87) [41].

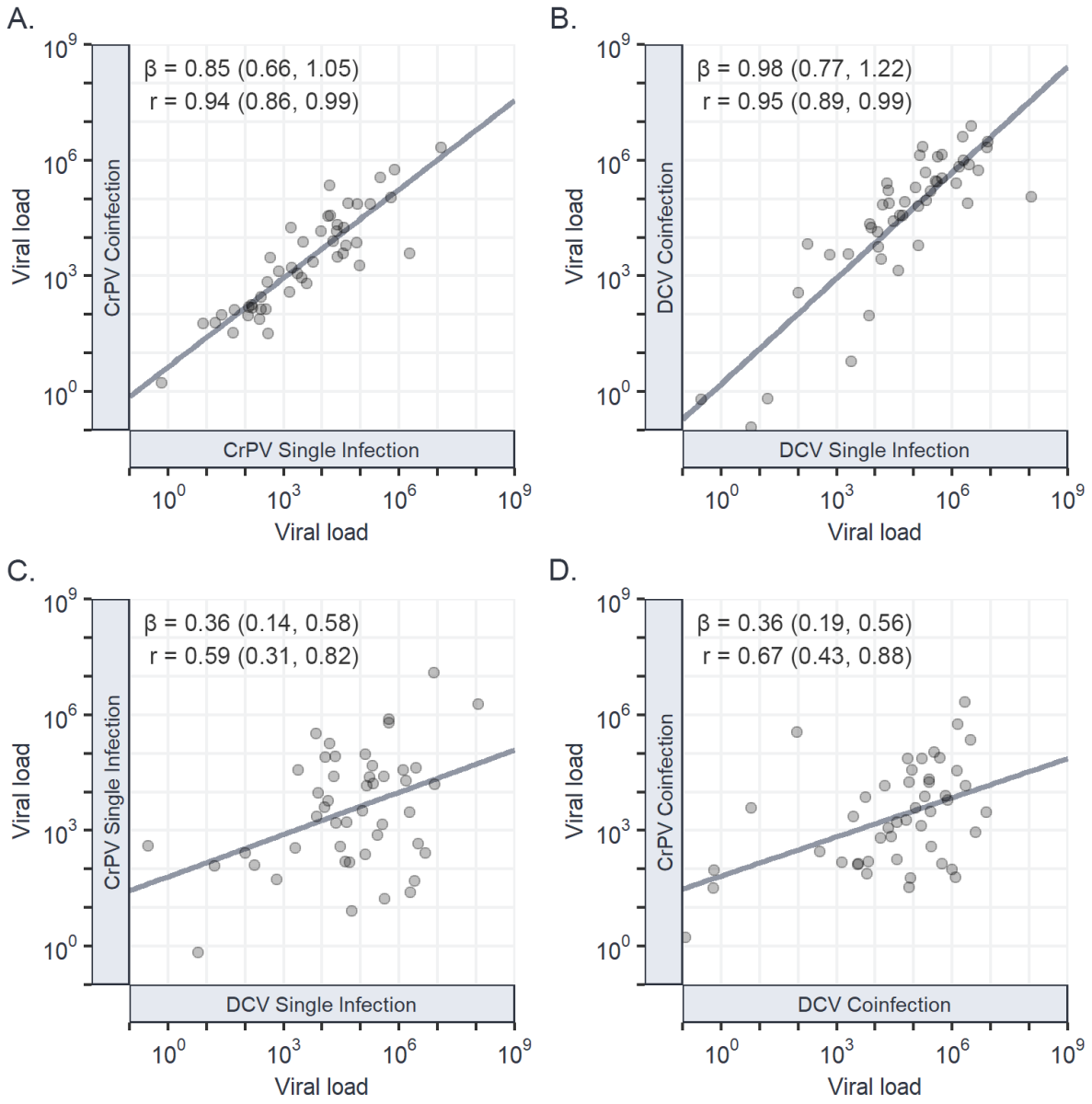

Figure 4: Interspecific correlations in viral load between single and coinfections of CrPV and DCV. Correlations in viral load between CrPV during single and coinfection (A); DCV during single and coinfection (B); CrPV and DCV during single infection (C); and CrPV and DCV during coinfection (D). Individual points represent the mean viral load at 2 dpi for each *Drosophilidae* host species on a $\log_{10}$ scale, with trend lines added from a univariate least-squares linear model for illustrative purposes. Interspecific correlations (r), regression slopes (β), and 95% CIs have been taken from the output of model (4).

Little evidence of phylogenetic signal in the strength of coinfection interaction

As the viral loads of DCV and CrPV show a strong phylogenetic signal across host species, we also tested if there was phylogenetic signal across hosts in the change in viral load from single to coinfection (Table 2). Fitting phylogenetic mixed models to these data revealed little support for any phylogenetic signal in the change in viral load during coinfection, with low estimates of repeatability for DCV: 0.36 (0.08, 0.62) and no credible difference from zero for repeatability of CrPV or the variance explained by phylogeny for either virus.

Discussion

Here, we measured variation in the outcome of coinfections within and across host species, using a *Drosophila* experimental system and two *Cripaviruses*: DCV and CrPV. We found effects of coinfection on viral load across genotypes of *D. melanogaster*, with DCV increasing ~3 fold and CrPV decreasing ~2 fold during coinfection. Consistent with previous studies, we found that host genetic variation explained a large proportion of variation in susceptibility to single infections [64], but little evidence was found for a change in this genetic component of susceptibility in the presence of a coinfecting virus, or for a host genetic component to the strength of interaction between these viruses. Across host species, we found no evidence of consistent coinfection interactions between these viruses and no change in the phylogenetic patterns of susceptibility to each virus during coinfection, although coinfection interactions were apparent in a subset of host species. Strong positive correlations between single and coinfection viral loads, and between DCV and CrPV both within and across host species suggest that similar genetic architectures are underlying susceptibility to these viruses, and that susceptibility is largely independent of coinfection status.

Exploitative coinfection interactions – where one pathogen benefits from coinfection to the detriment of the other – have been described in intestinal parasites of wood mice and wild rabbits [90,91], and in mixed-genotype *Pseudomonas* infections in plants [92]. The mechanisms underlying exploitative coinfection interactions are unknown but may be due to differences in the relative importance of specific interactions between pathogens and the host in overall susceptibility. Within *D. melanogaster*, our data suggest that the strength of interaction between DCV and CrPV is not virus density-dependent, as more susceptible host

genotypes did not experience increased changes in viral load with coinfection compared to more resistant genotypes. This suggests that the coinfection interaction within *D. melanogaster* is unlikely to be caused by resource competition between DCV and CrPV, as susceptible hosts experienced >100-fold higher viral loads for both DCV and CrPV compared to more resistant hosts with no evidence of limited virus replication. DCV may instead be benefiting from increased suppression of antiviral RNAi due to expression of the CrPV immune inhibitor [62], while CrPV is hindered by the activation of other mechanisms of host immunity by DCV. However, complex direct virus-virus interactions have been described in multiple coinfections, and it is possible that DCV and CrPV are directly influencing each other's expression or virion surface composition [93,94].

Across host species, the changes in viral load during coinfection were highly variable and show no consistent interaction between DCV and CrPV. Coupled with the fact we did not detect effects of genetic variation within host species or evolutionary relatedness across host species in the change in viral load during coinfection, our results suggest that natural levels of variation in host genetics have little impact on the strength of interaction between these viruses during coinfection. This contrasts with coinfection studies in other systems, which describe variation between host genotypes in pathogen community composition, coinfection prevalence, and disease severity during coinfection [31–33]. Mathematical models investigating stochasticity during coinfection have suggested that otherwise identical coinfections can have directionally different outcomes [95], and so it may be that any influences of host evolutionary relatedness and genotype are being masked by high stochasticity in the outcome of coinfection in this system. Alternatively, variation in the strength of coinfection interaction between host genotypes may be influenced by a small number of major-effect loci that are not dispersed phylogenetically, which these experiments were not designed to detect.

As inferential and epidemiological models of cross-species infections grow in complexity, they will continue to incorporate more non-genomic data which is known to influence the outcome of infection (e.g., [96]). Our findings suggest that coinfection will not be a necessary inclusion in models of every host-pathogen system, as the ability of the host phylogeny to explain variation in viral load across host species was largely unaffected during coinfection in this case. Despite this, coinfection is known to cause changes in infection traits in many

539 systems [4–9,97–109], with consequences for pathogen spread and establishment in natural
540 populations [10–15]. Few studies exist that describe pathogens that do not interact during
541 coinfection [110] (although this may represent publication bias), and so the frequency of
542 consequential coinfection interactions in nature is as yet unknown . It remains unclear if
543 interactions between pathogens can be consistently predicted *a priori* from single infection
544 data [111,112], or from pathogen and host genomic data [113]. In cases of direct interaction
545 between pathogens, such as the binding and activation of endogenous HIV by herpes
546 simplex virus proteins [93], differing outcomes in coinfection may be predictable through
547 conventional tools for inferring protein-protein and protein-nucleotide binding [114,115].
548 However, where pathogens interact indirectly, such as through immune modulation or
549 resource availability, it may be necessary to understand the extent of variation in these host
550 factors that is required to influence the outcome of infection before inferring interactions
551 between coinfecting pathogens.

552

553 Here, we have tested for variation in the outcome of coinfection within and across host
554 species, and our findings suggest that host genetics may not influence coinfection
555 interactions in all host-pathogen systems. This approach can now be expanded to a more
556 diverse range of coinfecting pathogens, to look for effects of host genetic variation during
557 other pathogen-pathogen interactions, to better understand the potential determinants of the
558 outcome of coinfection interactions, and how these interactions may affect the evolution of
559 host susceptibility.
560

561 **Acknowledgements**

562 We would like to thank Camille Bonneaud and Ann Tate for useful discussion. Ben Longdon
563 and Ryan M. Imrie are supported by a Sir Henry Dale Fellowship jointly funded by the
564 Wellcome Trust and the Royal Society (grant no. 109356/Z/15/Z), and a studentship funded
565 by the Natural Environment Research Council (NERC) GW4+ Doctoral Training Partnership.
566 Sarah K. Walsh is funded by a studentship from the Biotechnology and Biological Sciences
567 Research Council (BBSRC) South West Biosciences Doctoral Training Partnership
568 (BB/M009122/1). For the purpose of Open Access, the author has applied a CC BY public
569 copyright licence to any Author Accepted Manuscript version arising from this submission.

570

References

1. Read AF, Taylor LH. The Ecology of Genetically Diverse Infections. Science. 2001;292(5519):1099–102. doi: 10.1126/science.1059410
2. Petney TN, Andrews RH. Multiparasite communities in animals and humans: frequency, structure and pathogenic significance. Int J Parasitol. 1998;28(3):377–93. doi: 10.1016/s0020-7519(97)00189-6
3. Cox FEG. Concomitant infections, parasites and immune responses. Parasitology. 2001;122(S1):S23–38. doi: 10.1017/s003118200001698x
4. Harrison F, Browning LE, Vos M, Buckling A. Cooperation and virulence in acute Pseudomonas aeruginosa infections. Bmc Biol. 2006;4(1):21. doi: 10.1186/1741-7007-4-21
5. Loving CL, Brockmeier SL, Vincent AL, Palmer MV, Sacco RE, Nicholson TL. Influenza virus coinfection with Bordetella bronchiseptica enhances bacterial colonization and host responses exacerbating pulmonary lesions. Microb Pathogenesis. 2010;49(5):237–45. doi: 10.1016/j.micpath.2010.06.004
6. Karvonen A, Rellstab C, Louhi K-R, Jokela J. Synchronous attack is advantageous: mixed genotype infections lead to higher infection success in trematode parasites. Proc Royal Soc B Biological Sci. 2012;279(1726):171–6. doi: 10.1098/rspb.2011.0879
7. Kalhoro DH, Gao S, Xie X, Liang S, Luo S, Zhao Y et al. Canine influenza virus coinfection with Staphylococcus pseudintermedius enhances bacterial colonization, virus load and clinical presentation in mice. Bmc Vet Res. 2016;12(1):87. doi: 10.1186/s12917-016-0708-6
8. Lass S, Hudson PJ, Thakar J, Saric J, Harvill E, Albert R et al. Generating super-shedders: co-infection increases bacterial load and egg production of a gastrointestinal helminth. J Roy Soc Interface. 2013;10(80):20120588. doi: 10.1098/rsif.2012.0588
9. Basso M, Andreis S, Scaggiante R, Franchin E, Zago D, Biasolo MA et al. Cytomegalovirus, Epstein-Barr virus and human herpesvirus 8 salivary shedding in HIV positive men who have sex with men with controlled and uncontrolled plasma HIV viremia: a 24-month longitudinal study. Bmc Infect Dis. 2018;18(1):683. doi: 10.1186/s12879-018-3591-x
10. Ezenwa VO, Jolles AE. From Host Immunity to Pathogen Invasion: The Effects of Helminth Coinfection on the Dynamics of Microparasites. Integr Comp Biol. 2011;51(4):540–51. doi: 10.1093/icb/icr058
11. Abu-Raddad LJ, Patnaik P, Kublin JG. Dual Infection with HIV and Malaria Fuels the Spread of Both Diseases in Sub-Saharan Africa. Science. 2006;314(5805):1603–6. doi: 10.1126/science.1132338
12. Nickbakhsh S, Mair C, Matthews L, Reeve R, Johnson PCD, Thorburn F et al. Virus–virus interactions impact the population dynamics of influenza and the common cold. P Natl Acad Sci Usa. 2019;116(52):27142–50. doi: 10.1073/pnas.1911083116
13. Mak GC, Wong AH, Ho WYY, Lim W. The impact of pandemic influenza A (H1N1) 2009 on the circulation of respiratory viruses 2009–2011. Influenza Other Resp. 2012;6(3):e6–10. doi: 10.1111/j.1750-2659.2011.00323.x
14. Xiridou M, Borkent-Raven B, Hulshof J, Wallinga J. How Hepatitis D Virus Can Hinder the Control of Hepatitis B Virus. Plos One. 2009;4(4):e5247. doi: 10.1371/journal.pone.0005247

15. Farci P, Niro G. Clinical Features of Hepatitis D. Semin Liver Dis. 2012;32(03):228–36. doi: 10.1055/s-0032-1323628
16. Seppälä O, Jokela J. Do Coinfections Maintain Genetic Variation in Parasites? Trends Parasitol. 2016;32(12):930–8. doi: 10.1016/j.pt.2016.08.010
17. Garbutt J, Bonsall MB, Wright DJ, Raymond B. Antagonistic competition moderates virulence in Bacillus thuringiensis. Ecol Lett. 2011;14(8):765–72. doi: 10.1111/j.1461-0248.2011.01638.x
18. Bhattacharya A, Díaz VCT, Morran LT, Bashey F. Evolution of increased virulence is associated with decreased spite in the insect-pathogenic bacterium Xenorhabdus nematophila. Biol Letters. 2019;15(8):20190432. doi: 10.1098/rsbl.2019.0432
19. Kümmerli R, Griffin AS, West SA, Buckling A, Harrison F. Viscous medium promotes cooperation in the pathogenic bacterium Pseudomonas aeruginosa. Proc Royal Soc B Biological Sci. 2009;276(1672):3531–8. doi: 10.1098/rspb.2009.0861
20. Ford SA, Kao D, Williams D, King KC. Microbe-mediated host defence drives the evolution of reduced pathogen virulence. Nat Commun. 2016;7(1):13430. doi: 10.1038/ncomms13430
21. Cressler CE, Nelson WA, Day T, McCauley E, Bonsall M. Disentangling the interaction among host resources, the immune system and pathogens. Ecol Lett. 2014;17(3):284–93. doi: 10.1111/ele.12229
22. Ramiro RS, Pollitt LC, Mideo N, Reece SE. Facilitation through altered resource availability in a mixed-species rodent malaria infection. Ecol Lett. 2016;19(9):1041–50. doi: 10.1111/ele.12639
23. Griffiths EC, Fairlie-Clarke K, Allen JE, Metcalf CJE, Graham AL. Bottom-up regulation of malaria population dynamics in mice co-infected with lung-migratory nematodes. Ecol Lett. 2015;18(12):1387–96. doi: 10.1111/ele.12534
24. Graham AL. Ecological rules governing helminth–microparasite coinfection. Proc National Acad Sci. 2008;105(2):566–70. doi: 10.1073/pnas.0707221105
25. Modjarrad K, Vermund SH. Effect of treating co-infections on HIV-1 viral load: a systematic review. Lancet Infect Dis. 2010;10(7):455–63. doi: 10.1016/s1473-3099(10)70093-1
26. Grivel J-C, Santoro F, Chen S, Fagá G, Malnati MS, Ito Y et al. Pathogenic Effects of Human Herpesvirus 6 in Human Lymphoid Tissue Ex Vivo. J Virol. 2003;77(15):8280–9. doi: 10.1128/jvi.77.15.8280-8289.2003
27. Lisco A, Grivel J-C, Biancotto A, Vanpouille C, Origgi F, Malnati MS et al. Viral Interactions in Human Lymphoid Tissue: Human Herpesvirus 7 Suppresses the Replication of CCR5-Tropic Human Immunodeficiency Virus Type 1 via CD4 Modulation. J Virol. 2007;81(2):708–17. doi: 10.1128/jvi.01367-06
28. King CA, Baillie J, Sinclair JH. Human cytomegalovirus modulation of CCR5 expression on myeloid cells affects susceptibility to human immunodeficiency virus type 1 infection. J Gen Virol. 2006;87(8):2171–80. doi: 10.1099/vir.0.81452-0
29. Biancotto A, Iglehart SJ, Lisco A, Vanpouille C, Grivel J-C, Lurain NS et al. Upregulation of Human Cytomegalovirus by HIV Type 1 in Human Lymphoid Tissue ex Vivo. Aids Res Hum Retrov. 2008;24(3):453–62. doi: 10.1089/aid.2007.0155
30. Grivel J-C, García M, Moss WJ, Margolis LB. Inhibition of HIV-1 Replication in Human Lymphoid Tissues Ex Vivo by Measles Virus. J Infect Dis. 2005;192(1):71–8. doi:

10.1086/430743
31. Susi H, Barrès B, Vale PF, Laine A-L. Co-infection alters population dynamics of infectious disease. Nat Commun. 2015;6(1):5975. doi: 10.1038/ncomms6975
32. Susi H, Laine A. Host resistance and pathogen aggressiveness are key determinants of coinfection in the wild. Evolution. 2017;71(8):2110–9. doi: 10.1111/evo.13290
33. Sallinen S, Norberg A, Susi H, Laine A-L. Intraspecific host variation plays a key role in virus community assembly. Nat Commun. 2020;11(1):5610. doi: 10.1038/s41467-020-19273-z
34. Randall J, Cable J, Guschina IA, Harwood JL, Lello J. Endemic infection reduces transmission potential of an epidemic parasite during co-infection. Proc Royal Soc B Biological Sci. 2013;280(1769):20131500. doi: 10.1098/rspb.2013.1500
35. Lange B, Reuter M, Ebert D, Muylaert K, Decaestecker E. Diet quality determines interspecific parasite interactions in host populations. Ecol Evol. 2014;4(15):3093–102. doi: 10.1002/ece3.1167
36. Berg L van den, Henneman P, Dijk KW van, Waal HAD de, Oostra BA, Duijn CM van et al. Heritability of dietary food intake patterns. Acta Diabetol. 2013;50(5):721–6. doi: 10.1007/s00592-012-0387-0
37. Lopez-Minguez J, Dashti HS, Madrid-Valero JJ, Madrid JA, Saxena R, Scheer FAJL et al. Heritability of the timing of food intake. Clin Nutr. 2019;38(2):767–73. doi: 10.1016/j.clnu.2018.03.002
38. Gilbert GS, Webb CO. Phylogenetic signal in plant pathogen–host range. Proc National Acad Sci. 2007;104(12):4979–83. doi: 10.1073/pnas.0607968104
39. Longdon B, Hadfield JD, Webster CL, Obbard DJ, Jiggins FM. Host Phylogeny Determines Viral Persistence and Replication in Novel Hosts. Plos Pathog. 2011;7(9):e1002260. doi: 10.1371/journal.ppat.1002260
40. Longdon B, Hadfield JD, Day JP, Smith SCL, McGonigle JE, Cogni R et al. The Causes and Consequences of Changes in Virulence following Pathogen Host Shifts. Plos Pathog. 2015;11(3):e1004728. doi: 10.1371/journal.ppat.1004728
41. Imrie RM, Roberts KE, Longdon B. Between virus correlations in the outcome of infection across host species: Evidence of virus by host species interactions. Evol Lett. 2021;5(5):472–83. doi: 10.1002/evl3.247
42. Roberts KE, Hadfield JD, Sharma MD, Longdon B. Changes in temperature alter the potential outcomes of virus host shifts. Plos Pathog. 2018;14(10):e1007185. doi: 10.1371/journal.ppat.1007185
43. Longdon B, Day JP, Alves JM, Smith SCL, Houslay TM, McGonigle JE et al. Host shifts result in parallel genetic changes when viruses evolve in closely related species. Plos Pathog. 2018;14(4):e1006951. doi: 10.1371/journal.ppat.1006951
44. Roberts KE, Longdon B. Viral susceptibility across host species is largely independent of dietary protein to carbohydrate ratios. J Evolution Biol. 2021;34(5):746–56. doi: 10.1111/jeb.13773
45. Mollentze N, Streicker DG, Murcia PR, Hampson K, Biek R. Virulence mismatches in index hosts shape the outcomes of cross-species transmission. Proc National Acad Sci. 2020;117(46):28859–66. doi: 10.1073/pnas.2006778117
46. Guth S, Visher E, Boots M, Brook CE. Host phylogenetic distance drives trends in virus virulence and transmissibility across the animal–human interface. Philosophical Transactions

705 Royal Soc B Biological Sci. 2019;374(1782):20190296. doi: 10.1098/rstb.2019.0296
706 47. Farrell MJ, Davies TJ. Disease mortality in domesticated animals is predicted by host
707 evolutionary relationships. Proc National Acad Sci. 2019;116(16):201817323. doi:
708 10.1073/pnas.1817323116
709 48. Albery GF, Eskew EA, Ross N, Olival KJ. Predicting the global mammalian viral sharing
710 network using phylogeography. Nat Commun. 2020;11(1):2260. doi: 10.1038/s41467-020-
711 16153-4
712 49. Shaw LP, Wang AD, Dylus D, Meier M, Pogacnik G, Dessimoz C et al. The phylogenetic
713 range of bacterial and viral pathogens of vertebrates. Mol Ecol. 2020;29(17):3361–79. doi:
714 10.1111/mec.15463
715 50. Davies TJ, Pedersen AB. Phylogeny and geography predict pathogen community
716 similarity in wild primates and humans. Proc Royal Soc B Biological Sci.
717 2008;275(1643):1695–701. doi: 10.1098/rspb.2008.0284
718 51. Streicker DG, Turmelle AS, Vonhof MJ, Kuzmin IV, McCracken GF, Rupprecht CE. Host
719 Phylogeny Constrains Cross-Species Emergence and Establishment of Rabies Virus in
720 Bats. Science. 2010;329(5992):676–9. doi: 10.1126/science.1188836
721 52. Marquis JF, Santos MJ, Teixeira CM, Batista MI, Cabral HN. Host-parasite relationships
722 in flatfish (Pleuronectiformes) – the relative importance of host biology, ecology and
723 phylogeny. Parasitology. 2011;138(1):107–21. doi: 10.1017/s0031182010001009
724 53. Carlson CJ, Farrell MJ, Grange Z, Han BA, Mollentze N, Phelan AL et al. The future of
725 zoonotic risk prediction. Philosophical Transactions Royal Soc B. 2021;376(1837):20200358.
726 doi: 10.1098/rstb.2020.0358
727 54. Geoghegan JL, Holmes EC. Predicting virus emergence amid evolutionary noise. Open
728 Biol. 2017;7(10):170189. doi: 10.1098/rsob.170189
729 55. Hellard E, Fouchet D, Vavre F, Pontier D. Parasite–Parasite Interactions in the Wild:
730 How To Detect Them? Trends Parasitol. 2015;31(12):640–52. doi: 10.1016/j.pt.2015.07.005
731 56. Wang X-H, Aliyari R, Li W-X, Li H-W, Kim K, Carthew R et al. RNA Interference Directs
732 Innate Immunity Against Viruses in Adult Drosophila. Science. 2006;312(5772):452–4. doi:
733 10.1126/science.1125694
734 57. Galiana-Arnoux D, Dostert C, Schneemann A, Hoffmann JA, Imler J-L. Essential
735 function in vivo for Dicer-2 in host defense against RNA viruses in drosophila. Nat Immunol.
736 2006;7(6):590–7. doi: 10.1038/ni1335
737 58. Goto A, Okado K, Martins N, Cai H, Barbier V, Lamiable O et al. The Kinase IKKβ
738 Regulates a STING- and NF-κB-Dependent Antiviral Response Pathway in Drosophila.
739 Immunity. 2018;49(2):225-234.e4. doi: 10.1016/j.immuni.2018.07.013
740 59. Sansone CL, Cohen J, Yasunaga A, Xu J, Osborn G, Subramanian H et al. Microbiota-
741 Dependent Priming of Antiviral Intestinal Immunity in Drosophila. Cell Host Microbe.
742 2015;18(5):571–81. doi: 10.1016/j.chom.2015.10.010
743 60. Costa A, Jan E, Sarnow P, Schneider D. The Imd Pathway Is Involved in Antiviral
744 Immune Responses in Drosophila. Plos One. 2009;4(10):e7436. doi:
745 10.1371/journal.pone.0007436
746 61. Rij RP van, Saleh M-C, Berry B, Foo C, Houk A, Antoniewski C et al. The RNA silencing
747 endonuclease Argonaute 2 mediates specific antiviral immunity in Drosophila melanogaster.
748 Gene Dev. 2006;20(21):2985–95. doi: 10.1101/gad.1482006
749 62. Nayak A, Berry B, Tassetto M, Kunitomi M, Acevedo A, Deng C et al. Cricket paralysis

750 virus antagonizes Argonaute 2 to modulate antiviral defense in Drosophila. Nat Struct Mol
751 Biol. 2010;17(5):547–54. doi: 10.1038/nsmb.1810
752 63. Chtarbanova S, Lamiable O, Lee K-Z, Galiana D, Troxler L, Meignin C et al. Drosophila
753 C Virus Systemic Infection Leads to Intestinal Obstruction. J Virol. 2014;88(24):14057–69.
754 doi: 10.1128/jvi.02320-14
755 64. Magwire MM, Fabian DK, Schweyen H, Cao C, Longdon B, Bayer F et al. Genome-
756 Wide Association Studies Reveal a Simple Genetic Basis of Resistance to Naturally
757 Coevolving Viruses in Drosophila melanogaster. Plos Genet. 2012;8(11):e1003057. doi:
758 10.1371/journal.pgen.1003057
759 65. Cao C, Cogni R, Barbier V, Jiggins FM. Complex Coding and Regulatory
760 Polymorphisms in a Restriction Factor Determine the Susceptibility of Drosophila to Viral
761 Infection. Genetics. 2017;206(4):2159–73. doi: 10.1534/genetics.117.201970
762 66. Cogni R, Cao C, Day JP, Bridson C, Jiggins FM. The genetic architecture of resistance
763 to virus infection in Drosophila. Mol Ecol. 2016;25(20):5228–41. doi: 10.1111/mec.13769
764 67. Martins NE, Faria VG, Nolte V, Schlötterer C, Teixeira L, Sucena É et al. Host
765 adaptation to viruses relies on few genes with different cross-resistance properties. Proc
766 National Acad Sci. 2014;111(16):5938–43. doi: 10.1073/pnas.1400378111
767 68. Drummond AJ, Suchard MA, Xie D, Rambaut A. Bayesian Phylogenetics with BEAUti
768 and the BEAST 1.7. Mol Biol Evol. 2012;29(8):1969–73. doi: 10.1093/molbev/mss075
769 69. Rambaut A, Drummond AJ, Xie D, Baele G, Suchard MA. Posterior Summarization in
770 Bayesian Phylogenetics Using Tracer 1.7. Systematic Biol. 2018;67(5):901–4. doi:
771 10.1093/sysbio/syy032
772 70. Yu G. Using ggtree to Visualize Data on Tree-Like Structures. Curr Protoc Bioinform.
773 2020;69(1):e96. doi: 10.1002/cpbi.96
774 71. Martinez J, Bruner-Montero G, Arunkumar R, Smith SCL, Day JP, Longdon B et al.
775 Virus evolution in Wolbachia-infected Drosophila. Proc Royal Soc B.
776 2019;286(1914):20192117. doi: 10.1098/rspb.2019.2117
777 72. Johnson KN, Christian PD. Molecular Characterization of Drosophila C Virus Isolates. J
778 Invertebr Pathol. 1999;73(3):248–54. doi: 10.1006/jipa.1998.4830
779 73. Johnson KN, Christian PD. A molecular taxonomy for cricket paralysis virus including
780 two new isolates from Australian populations ofDrosophila (Diptera: Drosophilidae). Arch
781 Virol. 1996;141(8):1509–22. doi: 10.1007/bf01718251
782 74. Drosophila Ringer's solution. Cold Spring Harbor Protocols. 2007; doi:
783 10.1101/pdb.rec10919
784 75. Short SM, Lazzaro BP. Female and male genetic contributions to post-mating immune
785 defence in female Drosophila melanogaster. Proc Royal Soc B Biological Sci.
786 2010;277(1700):3649–57. doi: 10.1098/rspb.2010.0937
787 76. Duneau DF, Kondolf HC, Im JH, Ortiz GA, Chow C, Fox MA et al. The Toll pathway
788 underlies host sexual dimorphism in resistance to both Gram-negative and Gram-positive
789 bacteria in mated Drosophila. Bmc Biol. 2017;15(1):124. doi: 10.1186/s12915-017-0466-3
790 77. Schwenke RA, Lazzaro BP. Juvenile Hormone Suppresses Resistance to Infection in
791 Mated Female Drosophila melanogaster. Curr Biol. 2017;27(4):596–601. doi:
792 10.1016/j.cub.2017.01.004
793 78. Landum M, Silva MS, Martins N, Teixeira L. Viral route of infection determines the effect
794 of Drosophila melanogaster gut bacteria on host resistance and

795 tolerance to disease. Biorxiv [Internet]. 2021 Jan 1;2021.02.18.431843. doi:
796 10.1101/2021.02.18.431843 Available from:
797 http://biorxiv.org/content/early/2021/02/18/2021.02.18.431843.abstract
798 79. Ruijter JM, Thygesen HH, Schoneveld OJ, Das AT, Berkhout B, Lamers WH. Factor
799 correction as a tool to eliminate between-session variation in replicate experiments:
800 application to molecular biology and retrovirology. Retrovirology. 2006;3(1):2. doi:
801 10.1186/1742-4690-3-2
802 80. Ruijter JM, Villalba AR, Hellemans J, Untergasser A, Hoff MJB van den. Removal of
803 between-run variation in a multi-plate qPCR experiment. Biomol Detect Quantification.
804 2015;5:10–4. doi: 10.1016/j.bdq.2015.07.001
805 81. Hadfield JD. MCMC Methods for Multi-Response Generalized Linear Mixed Models: The
806 MCMCglmm R Package. Journal of Statistical Software [Internet]. 2010;33(2):1–22.
807 Available from: http://www.jstatsoft.org/v33/i02/
808 82. Gilchrist GW, Huey RB, Serra L. Rapid evolution of wing size clines in Drosophila
809 subobscura. Genetica. 2001;112–113(1):273–86. doi: 10.1023/a:1013358931816
810 83. Huey RB, Moreteau B, Moreteau J-C, Gibert P, Gilchrist GW, Ives AR et al. Sexual size
811 dimorphism in a Drosophila clade, the D. obscura group. Zoology. 2006;109(4):318–30. doi:
812 10.1016/j.zool.2006.04.003
813 84. Freckleton RP, Harvey PH, Pagel M. Phylogenetic Analysis and Comparative Data: A
814 Test and Review of Evidence. Am Nat. 2002;160(6):712–26. doi: 10.1086/343873
815 85. Hansen TF, Pélabon C, Houle D. Heritability is not Evolvability. Evol Biol.
816 2011;38(3):258. doi: 10.1007/s11692-011-9127-6
817 86. Pagel M. Inferring the historical patterns of biological evolution. Nature.
818 1999;401(6756):877–84. doi: 10.1038/44766
819 87. Housworth EA, Martins EP, Lynch M. The Phylogenetic Mixed Model. Am Nat.
820 2004;163(1):84–96. doi: 10.1086/380570
821 88. Falconer D. Introduction to quantitative genetics. 4th ed. Pearson Education India; 1996.
822 89. Kim BY, Wang JR, Miller DE, Barmina O, Delaney E, Thompson A et al. Highly
823 contiguous assemblies of 101 drosophilid genomes. Elife. 2021;10:e66405. doi:
824 10.7554/elife.66405
825 90. Clerc M, Devevey G, Fenton A, Pedersen AB. Antibodies and coinfection drive variation
826 in nematode burdens in wild mice. Int J Parasitol. 2018;48(9–10):785–92. doi:
827 10.1016/j.ijpara.2018.04.003
828 91. Lello J, Boag B, Fenton A, Stevenson IR, Hudson PJ. Competition and mutualism
829 among the gut helminths of a mammalian host. Nature. 2004;428(6985):840–4. doi:
830 10.1038/nature02490
831 92. Barrett LG, Bell T, Dwyer G, Bergelson J. Cheating, trade-offs and the evolution of
832 aggressiveness in a natural pathogen population. Ecol Lett. 2011;14(11):1149–57. doi:
833 10.1111/j.1461-0248.2011.01687.x
834 93. Perre PV de, Segondy M, Foulongne V, Ouedraogo A, Konate I, Huraux J-M et al.
835 Herpes simplex virus and HIV-1: deciphering viral synergy. Lancet Infect Dis. 2008;8(8):490–
836 7. doi: 10.1016/s1473-3099(08)70181-6
837 94. Haney J, Vijayakrishnan S, Streetley J, Dee K, Goldfarb DM, Clarke M et al. Coinfection
838 by influenza A virus and respiratory syncytial virus produces hybrid virus particles. Nat
839 Microbiol. 2022;7(11):1879–90. doi: 10.1038/s41564-022-01242-5

95. Pinky L, Gonzalez-Parra G, Dobrovolny HM. Effect of stochasticity on coinfection dynamics of respiratory viruses. Bmc Bioinformatics. 2019;20(1):191. doi: 10.1186/s12859-019-2793-6

96. Brierley L, Pedersen AB, Woolhouse MEJ. Tissue tropism and transmission ecology predict virulence of human RNA viruses. Plos Biol. 2019;17(11):e3000206. doi: 10.1371/journal.pbio.3000206

97. Brealey JC, Chappell KJ, Galbraith S, Fantino E, Gaydon J, Tozer S et al. Streptococcus pneumoniae colonization of the nasopharynx is associated with increased severity during respiratory syncytial virus infection in young children. Respirol Carlton Vic. 2018;23(2):220–7. doi: 10.1111/resp.13179

98. Garcia-Garcia ML, Calvo C, Ruiz S, Pozo F, Pozo V del, Remedios L et al. Role of viral coinfections in asthma development. Plos One. 2017;12(12):e0189083. doi: 10.1371/journal.pone.0189083

99. Waknine-Grinberg JH, Gold D, Ohayon A, Flescher E, Heyfets A, Doenhoff MJ et al. Schistosoma mansoni infection reduces the incidence of murine cerebral malaria. Malaria J. 2010;9(1):5–5. doi: 10.1186/1475-2875-9-5

100. Yoshida L-M, Suzuki M, Nguyen HA, Le MN, Vu TD, Yoshino H et al. Respiratory syncytial virus: co-infection and paediatric lower respiratory tract infections. Eur Respir J. 2013;42(2):461–9. doi: 10.1183/09031936.00101812

101. Bo-shun Z, Li L, Qian Z, Zhen W, Peng Y, Guo-dong Z et al. Co-infection of H9N2 influenza virus and Pseudomonas aeruginosa contributes to the development of hemorrhagic pneumonia in mink. Vet Microbiol. 2020;240:108542. doi: 10.1016/j.vetmic.2019.108542

102. Pomorska-Mól M, Dors A, Kwit K, Kowalczyk A, Stasiak E, Pejsak Z. Kinetics of single and dual infection of pigs with swine influenza virus and Actinobacillus pleuropneumoniae. Vet Microbiol. 2017;201:113–20. doi: 10.1016/j.vetmic.2017.01.011

103. Bandilla M, Valtonen ET, Suomalainen L-R, Aphalo PJ, Hakalahti T. A link between ectoparasite infection and susceptibility to bacterial disease in rainbow trout. Int J Parasitol. 2006;36(9):987–91. doi: 10.1016/j.ijpara.2006.05.001

104. Righetti AA, Glinz D, Adiossan LG, Koua A-YG, Niamké S, Hurrell RF et al. Interactions and Potential Implications of Plasmodium falciparum-Hookworm Coinfection in Different Age Groups in South-Central Côte d'Ivoire. Plos Neglect Trop D. 2012;6(11):e1889. doi: 10.1371/journal.pntd.0001889

105. Mahana O, Arafa A-S, Erfan A, Hussein HA, Shalaby MA. Pathological changes, shedding pattern and cytokines responses in chicks infected with avian influenza-H9N2 and/or infectious bronchitis viruses. Virusdisease. 2019;30(2):279–87. doi: 10.1007/s13337-018-00506-1

106. Fondong VN, Pita JS, Rey MEC, Kochko A de, Beachy RN, Fauquet CM. Evidence of synergism between African cassava mosaic virus and a new double-recombinant geminivirus infecting cassava in Cameroon. J Gen Virol. 2000;81(1):287–97. doi: 10.1099/0022-1317-81-1-287

107. Clerc M, Fenton A, Babayan SA, Pedersen AB. Parasitic nematodes simultaneously suppress and benefit from coccidian coinfection in their natural mouse host. Parasitology. 2019;146(8):1096–106. doi: 10.1017/s0031182019000192

108. Péréfarres F, Thébaud G, Lefeuvre P, Chiroleu F, Rimbaud L, Hoareau M et al.

885 Frequency-dependent assistance as a way out of competitive exclusion between two strains
886 of an emerging virus. Proc Royal Soc B Biological Sci. 2014;281(1781):20133374. doi:
887 10.1098/rspb.2013.3374
888 109. Salines M, Barnaud E, Andraud M, Eono F, Renson P, Bourry O et al. Hepatitis E virus
889 chronic infection of swine co-infected with Porcine Reproductive and Respiratory Syndrome
890 Virus. Vet Res. 2015;46(1):55. doi: 10.1186/s13567-015-0207-y
891 110. Andersson M, Scherman K, Råberg L. Multiple-Strain Infections of Borrelia afzelii : A
892 Role for Within-Host Interactions in the Maintenance of Antigenic Diversity? Am Nat.
893 2013;181(4):545–54. doi: 10.1086/669905
894 111. Lello J, McClure SJ, Tyrrell K, Viney ME. Predicting the effects of parasite co-infection
895 across species boundaries. Proc Royal Soc B Biological Sci. 2018;285(1874):20172610. doi:
896 10.1098/rspb.2017.2610
897 112. Lello J, Hussell T. Functional group/guild modelling of inter-specific pathogen
898 interactions: A potential tool for predicting the consequences of co-infection. Parasitology.
899 2008;135(7):825–39. doi: 10.1017/s0031182008000383
900 113. Fenton A, Viney ME, Lello J. Detecting interspecific macroparasite interactions from
901 ecological data: patterns and process. Ecol Lett. 2010;13(5):606–15. doi: 10.1111/j.1461-
902 0248.2010.01458.x
903 114. Yan J, Friedrich S, Kurgan L. A comprehensive comparative review of sequence-based
904 predictors of DNA- and RNA-binding residues. Brief Bioinform. 2015;17(1):88–105. doi:
905 10.1093/bib/bbv023
906 115. Keskin O, Tuncbag N, Gursoy A. Predicting Protein–Protein Interactions from the
907 Molecular to the Proteome Level. Chem Rev. 2016;116(8):4884–909. doi:
908 10.1021/acs.chemrev.5b00683